

A Measurement Set Partitioning Algorithm Based on CFSFDP for Multiple Extended Target Tracking in PHD Filter

Yang GONG, Chen CUI

Institute of Electronic Countermeasure, National University of Defense Technology, Hefei 230037, China

Gongyang17@nudt.edu.cn, kycuichen@163.com

Submitted August 26, 2020 / Accepted April 2, 2021

Abstract. *The extended target probability hypothesis density (ET-PHD) filter is a promising approach for multiple extended target tracking. One crucial problem of the ET-PHD filter is partitioning the measurement set. This paper proposes a partitioning algorithm based on clustering by fast search and find density peaks (CFSFDP). Firstly, we adopt CFSFDP algorithm to partition the measurement set and the field theory is introduced to determine the cutoff distance of the CFSFDP algorithm. Then, the cluster center of the CFSFDP algorithm is determined according to solved cutoff distance and measurement rate. Finally, as the CFSFDP algorithm cannot handle the case in which targets are spatially close, an improved sub-partitioning method is implemented. Simulation results show that the proposed algorithm has less computational complexity and stronger robustness than the existing algorithm without losing tracking performance.*

Keywords

Probability hypothesis density filter, extended target tracking, measurement set, cutoff distance, sub-partitioning

1. Introduction

In target tracking, the target echo signal may be occupied in different range resolution cells. The sensor will receive multiple measurements from a target per scan and such target is referred to as an extended target [1]. In recent years, multiple extended target tracking has been hot research in the target tracking field [2], [3].

In multiple extended target tracking, the conventional algorithms, such as joint probabilistic data association (JPDA) and multiple hypothesis tracker (MHT), burden exploded computational complexity. Based on the probability hypothesis density (PHD) filter in [4], Mahler presented an extension of the PHD filter to multiple extended target tracking, which is called the extended target PHD (ET-PHD) filter [5]. The ET-PHD filter avoids the data

association and reduces computational complexity. Two main implementations for the ET-PHD filter are given in [6], [7], called the extended target Gaussian Mixture PHD (ET-GM-PHD) filter and the extended target particle PHD (ET-P-PHD) filter, respectively.

The key challenge of the ET-PHD filter is partitioning the measurement set rapidly and correctly. Therefore, various partitioning algorithms have been proposed. In [6], K-means++ algorithm is applied to partition the measurement set, but it needs the prior information of cluster number, and the partitioning results will become worse in a cluttered scene. In [8], distance partitioning is adopted to partition the measurement set. To get the correct partition, a large number of distance thresholds are needed. With the increase in the measurements generated by a target, distance partitioning makes ET-PHD filter computationally intractable. Based on neural network and adaptive resonance theory (ART), a fast partitioning algorithm with fuzzy ART is proposed in [9]. Although it has fewer partitions and less computational complexity than K-means++ partitioning and distance partitioning, it is sensitive to vigilance thresholds and becomes rather poor in a densely cluttered scene. An effective partitioning method [10] is proposed using spectral clustering technique, where the clutter is eliminated from the measurement set. But this method also needs the prior information of cluster number. The affinity propagation (AP) clustering [11], [12] is introduced into the measurement set partitioning. Although the AP clustering reduces the computational complexity, it is influenced by the initial value of the similarity matrix. In [13], an adaptive partitioning approach is proposed. However, it needs distance partitioning to partition the measurement set first and burdens high computation. In [14], an improved fuzzy c-means (FCM) algorithm is proposed to partition the measurement set. This algorithm sets a probability threshold to estimate the target number and then partitions the measurement set. The partitions number is much fewer, but it correspondingly increases as the target number increases.

When targets are spatially close, the distance between measurements generated by the different targets is small.

These measurements may be partitioned into the same cell. It will lead to the underestimation of the target number. As a remedy, the sub-partitioning method is adopted in [6], [9]. The sub-partitioning method solves the underestimation of target number to some extent. However, the above sub-partitioning method will result in a large number of additional partitions when there are multiple pairs of close targets whose cells are merged wrongly. More additional partitions will lead to high computational complexity.

In [15], clustering by fast search and find density peaks (CFSFDP) algorithm is proposed for clustering. Compared with the conventional clustering algorithms, the CFSFDP algorithm needs neither the prior information of cluster number nor iteration and it can realize clustering rapidly. Therefore, this paper adopts the CFSFDP algorithm to partition the measurement set. The contributions are as follows:

- 1) Since the cutoff distance of the CFSFDP algorithm needs to be determined by user experience, the idea of data field is introduced to determine the cutoff distance.
- 2) The choice of the cluster center in CFSFDP algorithm is relied on the decision graph and it is not a real-time process for measurement set partitioning. A method which can choose the cluster center automatically by the solved cutoff distance and the measurement rate of the target is proposed.
- 3) An improved sub-partitioning method is proposed. The improved sub-partitioning method decreases the computation burden due to no additional partitions.

The remainder of this paper is organized as follows: Section 2 gives a brief introduction of the ET-PHD filter and the partitioning of the measurement set; the implementation of the proposed algorithm is provided in Sec. 3; numerical simulations are shown in Sec. 4; conclusions are presented in Sec. 5.

2. ET-PHD Filter and Partitioning the Measurement Set

2.1 Target Motion Model and Measurement Model

In an MTT system, we assume the unknown number of targets is N_k , and the target states set is $X_k = \{x_k^1, \dots, x_k^{N_k}\}$. x_k^i is referred to as the i th target state. The measurement set obtained at time k is $Z_k = \{z_k^1, \dots, z_k^{M_k}\}$. z_k^j is referred to as the j th measurement and M_k is the number of measurements. The target dynamic motion model is defined as

$$x_k^i = f(x_{k-1}^i) + w_k^i \tag{1}$$

where $f(\cdot)$ is the dynamic motion model function and w_k^i is Gaussian white noise with covariance matrix Q_k . Each target state evolves according to the same dynamic motion model independent of the other targets.

The number of measurements generated by each target at each time is a Poisson distributed random variable with rate $\gamma(x_k^i)$ [16]. $\gamma(\cdot)$ is referred to as the measurement rate of the target and it is a known non-negative function defined over the target state space. The target measurement model is defined as

$$z_k^j = h(x_k^i) + e_k^j \tag{2}$$

where $h(\cdot)$ is the measure model function and e_k^j is Gaussian white noise with covariance matrix R_k . Each target is assumed to give rise to measurements independently of the other targets.

2.2 ET-PHD Filter

The aim of multiple extended target tracking is to obtain an estimate of the target states $X_k = \{x_k^1, \dots, x_k^{N_k}\}$, given the measurement set $Z_k = \{z_k^1, \dots, z_k^{M_k}\}$ at time k . It can be achieved under the ET-PHD framework by propagating the predicted PHD and updated PHD. The predicted PHD and updated PHD can be expressed as [5], [6]

$$D_{k|k-1}(x) = \int p_{S,k}(\zeta) f_{k|k-1}(x|\zeta) D_{k-1|k-1}(\zeta) d\zeta + \int \beta_{k|k-1}(x|\zeta) D_{k-1|k-1}(\zeta) d\zeta + \gamma_k(x), \tag{3}$$

$$D_{k|k}(x) = L_{Z_k}(x) D_{k|k-1}(x) \tag{4}$$

where x is the target state. $D_{k|k-1}(x)$ and $D_{k|k}(x)$ are predicted PHD and updated PHD, respectively. $\beta_{k|k-1}(x|\zeta)$ and $\gamma_k(x)$ are the spawn target PHD and birth target PHD, respectively. $p_{S,k}(\zeta)$ is the probability of target survival and $L_{Z_k}(x)$ is the pseudo-likelihood function, which can be expressed as

$$L_{Z_k}(x) = 1 - (1 - e^{-\gamma(x)}) p_{D,k}(x) + e^{-\gamma(x)} p_{D,k}(x) \sum_{p \subset Z_k} \omega_p \sum_{W \in p} \frac{\gamma(x)^{|W|}}{d_W} \cdot \prod_{z_k \in W} \frac{\phi_{z_k}(x)}{\lambda_k c_k(z_k)} \tag{5}$$

$p_{D,k}(x)$ is the detection probability. λ_k is the average clutter number and $c_k(z_k)$ is the spatial distribution of the clutter. $p \subset Z_k$ denotes the p th non-empty partition subset of Z_k and $W \in p$ denotes the W th cell of the partition p . $|W|$ denotes the number of measurements in cell W . $\phi_{z_k}(x) = g_k(z_k|x)$ is the likelihood function for a single target. ω_p and d_W denote the coefficients for each partition p and cell W shown as

$$\omega_p = \frac{\prod_{W \in p} d_W}{\sum_{p' \subset Z_k} \prod_{W' \in p'} d_{W'}}, \tag{6}$$

$$d_W = \delta_{|W|,1} + D_{k|k-1} \left[e^{-\gamma(x)} \gamma(x)^{|W|} p_{D,k}(x) \prod_{z_k \in W} \frac{\phi_{z_k}(x)}{\lambda_k c_k(z_k)} \right] \tag{7}$$

where $\delta_{i,j}$ is the Kronecker delta and $D_{k|k-1}[h] = \int h(x) D_{k|k-1}(x) dx$.

2.3 The Description of Partitioning the Measurement Set

As shown in (5), all the possible partitions of measurement set Z_k are needed in updated PHD. Assuming at time k , the measurement set Z_k contains three individual measurements, i.e., $Z_k = \{z_k^1, z_k^2, z_k^3\}$. Then all the possible partitions can be described as

$$\begin{aligned}
 p_1 : W_1^1 &= \{z_k^1, z_k^2, z_k^3\} \\
 p_2 : W_2^1 &= \{z_k^1, z_k^2\}, W_2^2 = \{z_k^3\} \\
 p_3 : W_3^1 &= \{z_k^1, z_k^3\}, W_3^2 = \{z_k^2\} \\
 p_4 : W_4^1 &= \{z_k^2, z_k^3\}, W_4^2 = \{z_k^1\} \\
 p_5 : W_5^1 &= \{z_k^1\}, W_5^2 = \{z_k^2\}, W_5^3 = \{z_k^3\}
 \end{aligned} \tag{8}$$

where p_i denotes the i th partition and W_i^j denotes the j th cell of partition i . It can be observed that as the number of measurements increases, the number of possible partitions grows sharply. When all the partitions are used for ET-PHD update, it will make ET-PHD filter computationally intractable. To reduce computational complexity, various measurement set partitioning algorithms have been proposed in [6–14]. They consider the most likely subset of all possible partitions to update the ET-PHD filter. The essence of the measurement set partitioning is the clustering problem. Distance partitioning, Kmeans++ partitioning, FCM partitioning and AP partitioning can be regarded as the clustering algorithms. In contrast, fuzzy ART can be regarded as a classification algorithm. Various partitioning algorithms have their own advantage and limitation. Although the above algorithms reduce the computational complexity to some extent, they still have the disadvantage of high computational complexity with the number of clutter and measurements increasing.

3. The Measurement Set Partitioning Algorithm Based on CFSFDP

3.1 CFSFDP Algorithm

As a clustering algorithm, CFSFDP algorithm calculates the local density ρ_i of each data point and its distance δ_i from points of higher density. The ρ_i and δ_i can be expressed as [15], [17]

$$\rho_i = \sum_j X(d_{ij} - d_c), \tag{9}$$

$$\delta_i = \begin{cases} \min(d_{ij}) & \text{if } \rho_j > \rho_i \\ \max(d_{ij}) & \text{others} \end{cases} \tag{10}$$

where d_{ij} is the distance between data point i and data point j , d_c is the cutoff distance. $X(x) = 1$ if $x \leq 0$ and $X(x) = 0$ otherwise. In CFSFDP algorithm, the cluster centers usually have a higher local density, and they are at a relatively

large distance from any points with higher local density. The outliers have a lower local density, and they are at a relatively large distance from any points with higher local density. After the cluster centers have been found and outliers have been removed, each remaining point is assigned to the same cluster as its nearest neighbor of higher density.

3.2 Determination of d_c and the Cluster Center

In this paper, we adopt CFSFDP algorithm to partition the measurement set. It can be seen from Sec. 3.1 that d_c has an impact on the calculation of the local density. In the conventional CFSFDP algorithm, d_c needs to be determined according to user experience. If d_c is too large, each measurement has a higher density. The measurements generated by different targets may be clustered together, leading to the underestimation of target number. In contrast, if d_c is too small, each measurement has a lower density. The measurements generated by the same target may be divided into multiple clusters, leading to the overestimation of target number. To avoid the blindness of empirical experience d_c , data field method is introduced to determine d_c adaptively.

In the data field, suppose that there is a dataset $X = \{x_1, x_2, \dots, x_n\}$ in a data space Ω . The potential function of an arbitrary data point x_i is defined as [18]

$$\varphi_i = \sum_{j=1}^n m_j \times K\left(\frac{\|x_j - x_i\|}{\sigma}\right) \tag{11}$$

where m_j is the mass of x_j , and σ is an impact factor. $K(x)$ is a unit potential function, and expresses the law how a data point diffuses its data contribution. $\|x_j - x_i\|$ is the distance between point i and point j . Since σ has a great impact on the distribution of data field, it is adaptively solved by minimizing the Shannon entropy of the potential as follows

$$\hat{\sigma} = \arg \min_{\sigma} H \tag{12}$$

where $H = -\sum_{i=1}^n \frac{\varphi_i}{Z} \log\left(\frac{\varphi_i}{Z}\right)$ is the Shannon entropy, and

$Z = \sum_{i=1}^{M_k} \varphi_i$ is the normalization factor.

In [19], the above method is introduced to extract the optimal cutoff distance of the CFSFDP algorithm when the local density is calculated by a Gaussian kernel. Similar to [19], we use (12) to determine the cutoff distance. Moreover, it can be seen from (2) that the measurements generated by a target are following Gaussian distribution. For Gaussian distribution, most data stochastically is distributed inside the interval between the expectation plus threefold variances and the expectation minus threefold variances [20]. So d_c in our paper is determined by

$$\hat{d}_c = \sqrt{3}\hat{\sigma} = \sqrt{3} \arg \min_{\sigma} H. \tag{13}$$

The objective function in (13) is a one-dimensional nonlinear function and it is solved by gradient descent method in this paper.

After \hat{d}_c is determined, ρ_i and δ_i of each measurement can be obtained by (9) and (10). Then, the cluster center is selected manually according to the decision graph of ρ_i and δ_i [15]. However, manual selection of the cluster center with the decision graph is not a real-time process for measurement set partitioning per time scan. Considering the cluster centers have a higher local density and higher distance, z_k^i can be treated as a cluster center if $\rho_i > \rho_c$ and $\delta_i > \delta_c$. ρ_c and δ_c are thresholds of density and distance, respectively.

We can see that δ_c reflects the distance between a cluster center and the adjacent measurement. Since \hat{d}_c can perfectly reflect the distribution of each measurement in the measurement set, we set $\delta_c = \hat{d}_c$ in this paper. ρ_c denotes the number of measurements near the cluster center, that is, the number of measurements generated by a target. Assume $\chi(x)$ is a constant, i.e., $\chi(x) = \gamma$. Let event A_γ^n denotes there are n measurements generated by a target with γ , and its probability is expressed as

$$P(A_\gamma^n) = \frac{\gamma^n}{n!} e^{-\gamma}. \tag{14}$$

The probability of A_γ^n is shown in Fig. 1 under different γ . In Fig. 1, it is clear that under a constant γ , $P(A_\gamma^n)$ approaches 0 when n is smaller. This indicates that the extended target is less likely to generate fewer measurements per scan. When γ becomes larger, n also becomes larger. Thus, we set a probability threshold p_{th1} in this paper and the corresponding measurements are regarded as originated-target measurements when the cumulative probability of $P(A_\gamma^i)$ is greater than p_{th1} . Therefore, ρ_c can be defined as

$$\rho_c = \arg \min_n \left\{ \sum_{i=0}^n P(A_\gamma^i) > p_{th1} \right\}. \tag{15}$$

According to (15), we can obtain ρ_c adaptively under different γ .

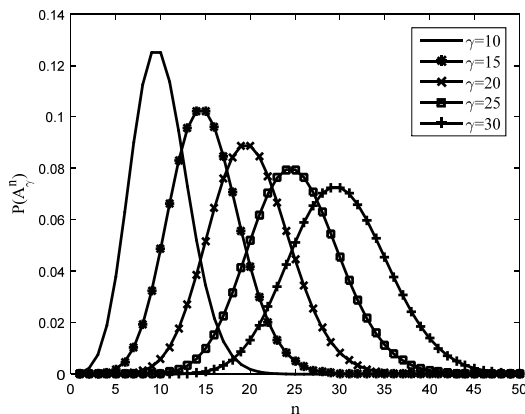


Fig. 1. The probability of A_γ^n under different γ .

3.3 Partitioning the Measurement Set

After the cluster center is determined, the measurement set Z_k can be partitioned by the CFSFDP algorithm. The detailed steps are shown in Tab. 1.

Input: $Z_k = \{z_k^1, \dots, z_k^{M_k}\}$, p_{th1} , and γ

Output: $p = \{\tilde{W}^j\}_{j=1}^{\tilde{N}}$

Step 1: Determine the cutoff distance d_c by (13) and calculate ρ_i and δ_i by (9) and (10).

Step 2: Determine ρ_c and δ_c . If $\rho_i \geq \rho_c$ and $\delta_i \geq \delta_c$, z_k^i is the cluster center.

Step 3: If $\rho_i < \rho_c$ and $\delta_i \geq \delta_c$, z_k^i is clutter.

Step 4: Remove all the clutter and assign the remaining measurements to the cluster.

Step 5: Get the partition $p = \{\tilde{W}^j\}_{j=1}^{\tilde{N}}$, where \tilde{N} is the number of cluster centers, and \tilde{W}^j is the j th partition cell.

Tab. 1. Partitioning the measurement set by CFSFDP algorithm.

Remark1: When the measurements generated by a target are relatively dispersed, these measurements may be partitioned into multiple cells with the above partitioning algorithm. The wrong cells will lead to the overestimation of the target number after ET-PHD filter update. To solve the overestimation of the target number, a merge operation is added after Step 5. Letting $d_{\tilde{m}\tilde{n}}$ denote the distance between cluster center $z_k^{\tilde{m}}$ and cluster center $z_k^{\tilde{n}}$, if $d_{\tilde{m}\tilde{n}} < \hat{d}_c$ is satisfied, $z_k^{\tilde{m}}$ and $z_k^{\tilde{n}}$ are more likely to be generated by the same target. We merge the corresponding cell $\tilde{W}^{\tilde{m}}$ and cell $\tilde{W}^{\tilde{n}}$ into one cell \tilde{W} , and the cluster center of \tilde{W} is the z_k^i with higher $\delta_i (i \in \{\tilde{m}, \tilde{n}\})$.

3.4 Sub-partitioning

When targets are spatially close, the distance between measurements generated by the different targets will be small. These measurements may be partitioned into the same cell which will lead to the underestimation of the target number. As a remedy, the sub-partitioning method is taken in [6], [9] to solve the problem. Assuming the measurements generated from different targets are independent, the likelihood function for the number of targets $N_{\tilde{W}^j}$ corresponding to the cell \tilde{W}^j in partition p can be expressed as [6]

$$p(|\tilde{W}^j| | N_{\tilde{W}^j}) = \frac{(\gamma N_{\tilde{W}^j})^{|\tilde{W}^j|}}{(|\tilde{W}^j|)!} e^{-(\gamma N_{\tilde{W}^j})}. \tag{16}$$

Assuming the number of clutter in cell \tilde{W}^j can be negligible, i.e. there is no clutter in \tilde{W}^j . The maximum likelihood (ML) estimate of $\hat{N}_{\tilde{W}^j}$ can be calculated as

$$\hat{N}_{\tilde{W}^j} = \arg \max_{N_{\tilde{W}^j}} p(|\tilde{W}^j| | N_{\tilde{W}^j}) = \frac{|\tilde{W}^j|}{\gamma}. \tag{17}$$

If $\hat{N}_{\tilde{W}^j} > 1$, the cell \tilde{W}^j is regarded as a wrong cell and the measurements in \tilde{W}^j are generated by $n_{\tilde{W}^j} = \text{ceil}(\hat{N}_{\tilde{W}^j})$ targets. $\text{ceil}(x)$ denotes the smallest integer more than x . An additional partition $p_l = p$ is added into the list of partitions and the cell \tilde{W}^j in partition p_l is split into $n_{\tilde{W}^j}$ smaller cells $\{W_s^+\}_{s=1}^{n_{\tilde{W}^j}}$ by K-means method. The original cell \tilde{W}^j in p_l is deleted. It can be seen that the above method solves the underestimation of the target number by identifying the wrong cell by $\hat{N}_{\tilde{W}^j} > 1$ and adding additional partitions. Therefore, multiple additional partitions are added when there are multiple wrong cells in one partition or there are wrong cells in multiple partitions. The added additional partitions will lead to high computational complexity.

To reduce the computational complexity, an improved sub-partitioning method is proposed. We can see from Fig. 1 that under the constant γ , $P(A_\gamma^n)$ approaches 0 when n is larger. Therefore, a probability threshold $p_{\text{th}2}$ is set, and we let

$$n_\gamma^{\min} = \arg \min_n \left\{ \sum_{i=0}^n P(A_\gamma^i) > p_{\text{th}2} \right\} \quad (18)$$

where n_γ^{\min} denotes the minimum number of measurements when the cumulative probability of the event A_γ^i is larger than $p_{\text{th}2}$. For the partition $p = \{\tilde{W}^j\}_{j=1}^N$, we calculate

$$N_\gamma^{\min} = \frac{|\tilde{W}^j|}{n_\gamma^{\min}}. \quad (19)$$

If $N_\gamma^{\min} > 1$, the \tilde{W}^j is treated as a wrong cell from $N_\gamma = \text{ceil}(N_\gamma^{\min})$ targets. As the classification result of K-means method depends on the choice of initial centers, the CFSFDP algorithm is used to split the wrong cell \tilde{W}^j . Sub-partitioning can be denoted as

$$\{W_s^+\}_{s=1}^{N_\gamma} = \text{CFSFDP}(\tilde{W}^j, N_\gamma). \quad (20)$$

Since the number of cluster centers is adaptively determined in CFSFDP algorithm, the estimate number \hat{N} may not always equal N_γ when the measurements generated by a target are relatively dispersed or clustered. Thus, a modification operation is implemented in this paper. If \hat{N} equals N_γ , \hat{N} centers are reserved as cluster centers of sub-partitioning directly. If \hat{N} is larger than N_γ , the center which has the largest $\hat{\delta}_i$ is selected as the first cluster center of sub-partitioning from \hat{N} centers. Then the distances between the first center and the $\hat{N} - 1$ remaining centers are calculated, and $N_\gamma - 1$ centers with larger distances are selected as the remaining cluster centers of sub-partitioning. If \hat{N} is smaller than N_γ , other $N_\gamma - \hat{N}$ centers should be added. The distance factor is considered for the new centers. We calculate the sum of distances between each measurement in \tilde{W}^j and \hat{N} centers, and $N_\gamma - \hat{N}$ measurements with larger distance sum are selected as added cluster centers of sub-partitioning. After the above steps, all N_γ cluster centers are selected.

When all the wrong cells in p are split, the wrong cells are removed and the split smaller cells are added into p . It can be seen that the improved sub-partitioning method makes use of the fact that the number of measurements generated by a target is Poisson distribution, which can be used to identify the wrong cells. The number of wrong cells will decrease, and the improved sub-partitioning method does not need to add the new partition which can reduce computational complexity.

Remark 2: It is worth noting that the \hat{d}_c should be recalculated when CFSFDP algorithm is performed to split cell \tilde{W}^j into N_γ smaller cells.

3.5 Computational Complexity Analysis

To demonstrate the performance of the proposed algorithm, we adopt K-means++ partitioning [6], distance partitioning [8], fuzzy ART partitioning [9], and FCM partitioning [14] as the compared algorithms. All the algorithms are implemented under the framework of ET-GM-PHD filter. In sub-partitioning, the compared algorithms adopt the sub-partitioning method in [6] and the proposed algorithm adopts the improved sub-partitioning method in this paper.

The computational complexity mainly contains two parts: the computational complexity of partitioning the measurement set and the computational complexity of update in ET-GM-PHD filter. For the computational complexity of partitioning the measurement set, the computational complexity of the distance partitioning in the worst case is approximated as $O(M_k^4)$ [21]. For K-means++ partitioning, the computational complexity is approximated as $O(\tau M_k^3)$, where τ is the iteration number. For fuzzy ART partitioning, the computational complexity is approximated as $O(256 \tau M_k^2 / \gamma)$ [9]. For FCM partitioning, the computational complexity is approximated as $O(\tau N_x \sum_{i=1}^P |p_i|)$. N_x is

the number of measurements after clutter removal, P is the number of partitions, and $|p_i|$ is the number of cells in partition p_i . For the proposed algorithm, the computational complexity mainly depends on the calculation of d_c , and its computational complexity is approximated as $O(\tau M_k^2)$.

For the computational complexity of update in ET-GM-PHD filter, the filter is updated by all cells in all partitions. The computational complexity of the five algorithms is approximated as $O(n_x^2 J_{k|k-1} \sum_{i=1}^P |p_i|)$. n_x is the dimension of

the target state vector and $J_{k|k-1}$ is the number of predicted Gaussian components. While P of fuzzy ART partitioning and FCM partitioning is much fewer than that of distance partitioning and K-means++ partitioning. For FCM partitioning, the clutter is eliminated and $|p_i|$ in each partition is much fewer than that of fuzzy ART partitioning. In contrast, the proposed algorithm has the only one partition and the clutter is eliminated. Its computational complexity is much less than that of FCM partitioning.

4. Simulations

4.1 Target Tracking Setup

Consider the multiple extended target tracking scenarios over the surveillance region $[-1000,1000] \times [-1000,1000](m^2)$. The target state vector $\mathbf{x}_k = [x_k, \dot{x}_k, y_k, \dot{y}_k]^T$ consists of position $[x_k, y_k]^T$ and velocity $[\dot{x}_k, \dot{y}_k]^T$. In order to verify the performance of the proposed algorithm, two scenarios are used. 50 Monte Carlo simulations are performed for each scenario. All the simulations are implemented in MATLAB 2015a with a PC (CPU Core i5 4GHz and 5GB RAM). The results are presented in terms of the target estimate number and optimal sub-pattern assignment (OSPA) [22] metric with the parameters $p = 2$ and $c = 100$.

The parameters of two scenarios are shown in Tab. 2. Clutter is uniformly distributed over the surveillance region. \mathbf{I}_2 denotes 2×2 identity matrix. $\sigma_v = 2 m/s^2$ is the standard deviation of the process noise, and $\sigma_e = 20 m$ is the standard deviation of measurement noise. In gradient descent method, iteration termination threshold is $\varepsilon = 0.001$, step length is $\zeta = 0.001$, and the maximum number of iteration is $\tau_{max} = 100$.

The birth PHD is described as

$$\gamma_k(x) = \sum_i 0.1 \mathcal{N}(x; \mathbf{m}_\gamma^i, \mathbf{P}_\gamma) \quad (21)$$

where $\mathbf{P}_\gamma = \text{diag}([100, 900, 100, 900])$, and \mathbf{m}_γ^i is initialized according to different tracking scenarios. The spawn target is not considered in the simulation.

Figure 2 shows the target theoretical tracks in two scenarios, where circles are the starting points and triangles are ending points. Scenario 1 has three targets, and the total time is 50 s. Three targets are over the surveillance region in 1~50 s, 10~40 s, and 20~50 s, respectively. Scenario 2 has three targets and the total time is 50 s. All three targets

Parameters	Value
State transfer matrix	$\mathbf{F}_k = \begin{bmatrix} 1 & \Delta & 0 & 0 \\ 0 & 1 & 0 & 0 \\ 0 & 0 & 1 & \Delta \\ 0 & 0 & 0 & 1 \end{bmatrix}$
Sampling period (s)	$\Delta = 1$
Process noise	$\mathbf{Q}_k = \sigma_v^2 \mathbf{I}_2$
Measurement matrix	$\mathbf{H}_k = \begin{bmatrix} 1 & 0 & 0 & 0 \\ 0 & 0 & 1 & 0 \end{bmatrix}$
Measurement noise	$\mathbf{R}_k = \sigma_e^2 \mathbf{I}_2$
Survival Probability	$P_{S,k} = 0.99$
Detection probability	$P_{D,k} = 0.99$
Measurement rate	$\gamma = 10$
Average clutter number	$\lambda_k = 10$
Thresholds	$p_{th1} = 0.005, p_{th2} = 0.95$

Tab. 2. Parameters of two scenarios.

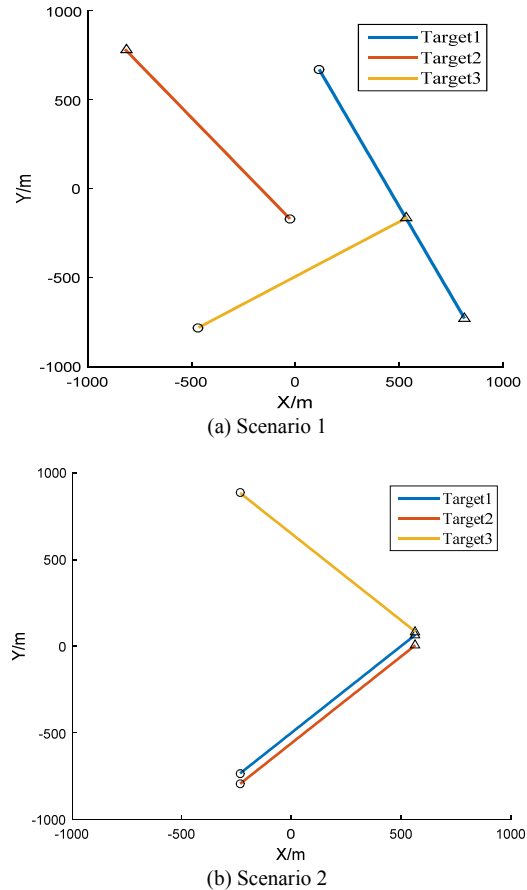
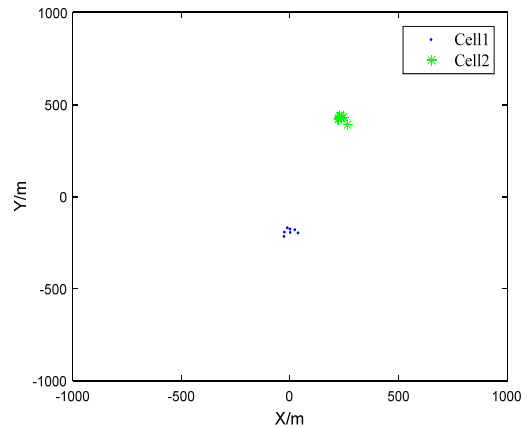


Fig. 2. Target theoretical tracks in two scenarios.

are over the surveillance region in 1~50 s. Target 1 and target 2 move in the same direction and keep 60 m apart all the time.

4.2 Simulation Result Analysis

Figure 3 gives the corresponding partitioning results with the proposed algorithm at times $k = 11$ and $k = 25$ in Scenario 1. At times $k = 11$ and $k = 25$, there are two targets and three targets, respectively. It can be seen that the proposed algorithm can divide the measurement set into two and three cells correctly.



(a) Partitioning result at time $k = 11$

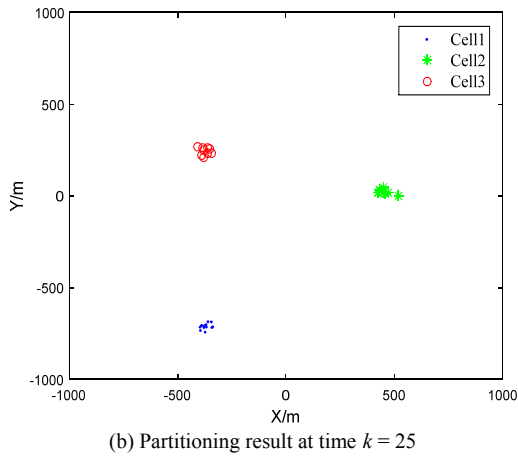


Fig. 3. Partitioning results with the proposed algorithm in Scenario 1.

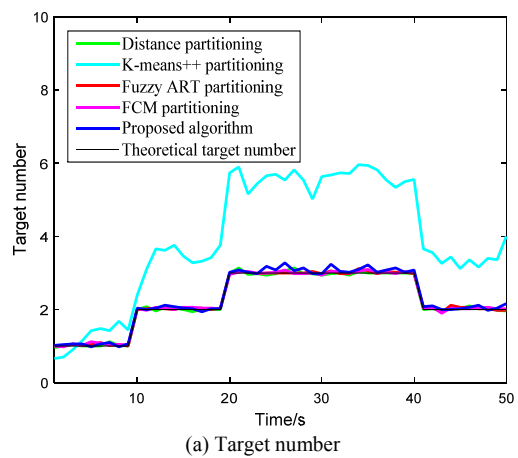


Fig. 4. Estimate of target number and OSPA in Scenario 1.

Figure 4 shows the estimate of the target number and OSPA in Scenario 1. It is clear that the estimate accuracy of the proposed algorithm approximately equals that of distance partitioning, fuzzy ART partitioning, and FCM partitioning, but it outperforms that of the K-means++ partitioning. This is because K-means++ partitioning often fails to obtain the correct partitions, and it partitions the measurements generated by a target into multiple cells [23], leading to the overestimation of the target number and larger OSPA.

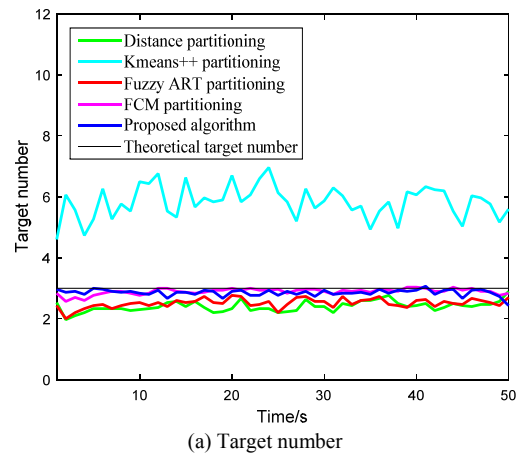


Fig. 5. Estimate of target number and OSPA in Scenario 2.

Figure 5 shows the estimate of target number and OSPA in Scenario 2. It can be seen that the K-means++ partitioning still performs worse than the other algorithms when targets are spatially close. Influenced by clutter and sub-partitioning, the target number is still underestimated for distance partitioning and fuzzy ART partitioning. The target number estimate of FCM partitioning has similar accuracy to that of the proposed algorithm. The proposed algorithm splits the wrong cells by CFSFDP algorithm, and it can get more accurate sub-cells, and has smaller OSPA than FCM partitioning.

Figure 6 shows the average run time of each step for five algorithms in two scenarios. In Scenario 1, the average run time of five algorithms is 5.07 s, 3.08 s, 0.37 s, 0.12 s, and 0.02 s, respectively. It can be seen that the average run time of five algorithms increases with the increase in target number. However, the average run time of the proposed algorithm is much less than that of the compared algorithms. In Scenario 2, the average run time of five algorithms is 17.19 s, 7.07 s, 0.49 s, 0.20 s, and 0.02 s, respectively. When targets are spatially close, the number of partitions for distance partitioning will increase due to more distance thresholds, which lead to the average run time increasing sharply. Meanwhile, for the compared algorithms, the number of partitions with wrong cells will increase. More additional partitions are added in sub-partitioning, which leads to higher computation. In contrast, the

proposed algorithm need not add the new partition in sub-partitioning and the average run time is approximately unchanged.

To further validate the performance of the proposed algorithm, in Scenario 1, the impact of different λ_k and different measure noise is analyzed. Figure 7 shows the estimate of the target number and OSPA for distance partitioning, fuzzy ART partitioning, FCM partitioning, and the proposed algorithm under different λ_k . It can be seen that at a higher clutter rate, the estimate error of fuzzy ART partitioning increases. The results are based on the fact that the detection threshold in fuzzy ART partitioning might be unreasonable in a densely cluttered scene. Thus, the target number will be overestimated, and OSPA becomes larger. Thus, the estimate error of distance partitioning also increases. Since the clutter is eliminated by elliptical gating in FCM partitioning, the identification of clutter is related to the target predicted location. When the target predicted location is not accurate, the clutter may be considered as the measurement generated by targets and is used for updating. This will increase the estimate error. The proposed algorithm removes the clutter by local density and distance, and it is not affected by the target predicted location. With the increase of λ_k , the proposed algorithm has approximately the same estimate performance and the estimate accuracy is the highest than the other algorithms.

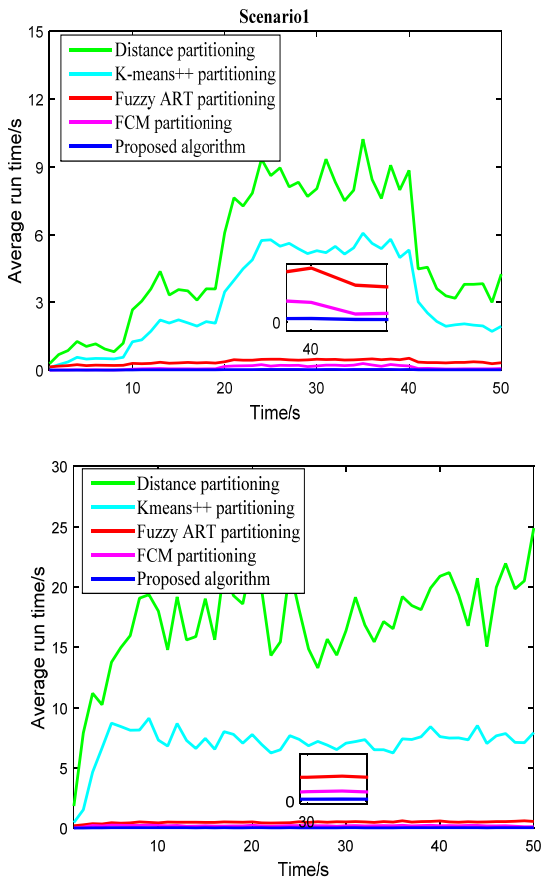


Fig. 6. Average run time of each step for five algorithms.

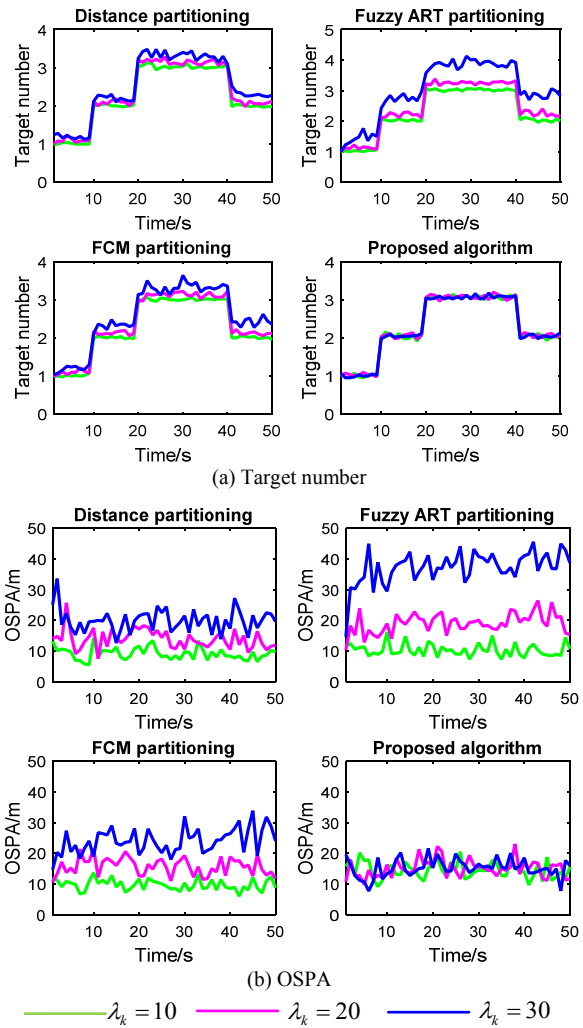


Fig. 7. Estimate of target number and OSPA under different λ_k .

Figure 8 shows the estimate of target number and OSPA of the proposed algorithm under different measurement noise. From Fig. 8, it can be seen that the estimate of target number keeps nearly the same. This is because the estimate of the target number relies on the accuracy of the partitioned measurement set, and the proposed algorithm could achieve the correct partition. With the measurement noise increasing, the estimate error of target state becomes larger which leads to the increase of OSPA. In general, the proposed algorithm has good performance under different λ_k and different measure noise, which reflects the strong robustness of the proposed algorithm.

5. Conclusions

In this paper, a measurement set partitioning algorithm based on CFSFDP is proposed for multiple extended target tracking in PHD filter. Based on the advantage of the CFSFDP algorithm, the measurement set can be partitioned rapidly and correctly. To avoid the blindness of empirical experience cutoff distance and cluster center, the Shannon entropy of potential for measurement set is used to solve the

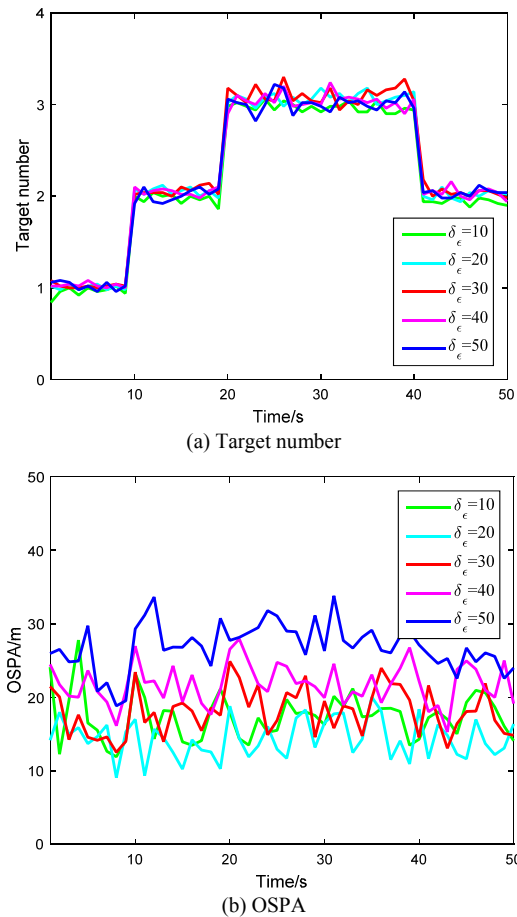


Fig. 8. Estimate of target number and OSPA under different measurement noise.

cutoff distance adaptively. Then, the cluster center is determined by the solved cutoff distance and measurement rate. In addition, an improved sub-partitioning method is proposed to deal with the case that the targets are spatially close. As the simulation results show, compared with the other partitioning algorithms, the proposed algorithm has lower computational complexity. Moreover, the proposed algorithm has stronger robustness under some challenging scenarios, such as high clutter rate and different measurement noise.

In the future works, we plan to apply the proposed algorithm to extended target Gaussian inverse wishart PHD (ET-GIW-PHD) filter in [13], [24]. Compared with ET-GM-PHD filter, the ET-GIW-PHD filter can estimate the target extension states. The proposed algorithm can also reduce the computation complexity of the ET-GIW-PHD filter.

References

[1] MAHLER, R. *Statistical Multisource-Multitarget Information Fusion*. Norwood (MA): Artech House, 2007. ISBN: 9781596930933

[2] LIU, M. Q., LAN, J. *Advanced Theory and Application of Target Tracking*. Science Press, 2015. (in Chinese). ISBN: 9787030426338

[3] LUNDQUIST, C., GRANSTROM, K., ORGUNER, U. An extended target CPD filter and a gamma Gaussian inverse Wishart implementation. *IEEE Journal of Selected Topics in Signal Processing*, 2013, vol. 7, no. 3, p. 472–483. DOI: 10.1109/JSTSP.2013.2245632

[4] MAHLER, R. Multitarget Bayes filtering via first-order multitarget moments. *IEEE Transactions on Aerospace and Electronic Systems*, 2003, vol. 39, no. 4, p. 1152–1178. DOI: 10.1109/TAES.2003.1261119

[5] MAHLER, R. PHD filters for nonstandard targets, I: Extended targets. In *Proceedings of the 12th International Conference on Information Fusion*. Seattle (WA, USA), July 2009, p. 915–921. ISBN: 9780982443804

[6] GRANSTROM, K., LUNDQUIST, C., ORGUNER, U. Extended target tracking using a Gaussian-mixture PHD filter. *IEEE Transactions on Aerospace and Electronic Systems*, 2012, vol. 48, no. 4, p. 3268–3286. DOI: 10.1109/TAES.2012.6324703

[7] LI, Y. X., XIAO, H. T., SONG, Z. Y., et al. A new multiple extended target tracking algorithm using PHD filter. *Signal Processing*, 2013, vol. 93, no. 12, p. 3578–3588. DOI: 10.1016/j.sigpro.2013.05.011

[8] GRANSTROM, K., LUNDQUIST, C., ORGUNER, U. A Gaussian mixture PHD filter for extended target tracking. In *Proceedings of the 13th International Conference on Information Fusion*. Edinburgh (Scotland, UK), July 2010, p. 1–8. DOI: 10.1109/ICIF.2010.5711885

[9] ZHANG, Y. Q., JI, H. B. A novel fast partitioning algorithm for extended target tracking using a Gaussian mixture PHD filter. *Signal Processing*, 2013, vol. 93, no. 11, p. 2975–2985. DOI: 10.1016/j.sigpro.2013.04.006

[10] YANG, J. L., LIU, F. M., GE, H. W., et al. Multiple extended target tracking algorithm based on GM-PHD filter and spectral clustering. *EURASIP Journal on Advances in Signal Processing*, 2014, p. 1–8. DOI: 10.1186/1687-6180-2014-117

[11] YANG, J. L., LIU, F. M., WANG, D., et al. Affinity propagation based measurement partition algorithm for multiple extended target tracking. *Journal of Radars*, 2015, vol. 4, no. 4, p. 452–459. (in Chinese) DOI:10.12000/JR15003

[12] ZHANG, T., WU, R. B. Affinity propagation clustering of measurements for multiple extended target tracking. *Sensors*, 2015, vol. 15, no. 9, p. 22646–22659. DOI: 10.3390/s150922646

[13] LI, P., GE, H. W., YANG, J. L. Adaptive measurement partitioning algorithm for a Gaussian inverse wishart PHD filter that tracks closely spaced extended targets. *Radioengineering*, 2017, vol. 26, no. 2, p. 573–580. DOI: 10.13164/re.2017.0573

[14] YAN, B., XU, N., XU, L. P., et al. An improved partitioning algorithm based on FCM algorithm for extended target tracking in PHD filter. *Digital Signal Processing*, 2019, vol. 90, p. 54–70. DOI: 10.1016/j.dsp.2019.04.002

[15] RODRIGUEZ, A., LAIO, A. Clustering by fast search and find of density peaks. *Science*, 2014, vol. 344, no. 6191, p. 1492–1496. DOI: 10.1126/science.1242072

[16] GILHOLM, K., GODSILL, S., MASKELL, S., et al. Poisson models for extended target and group tracking. In *Proceedings of Signal and Data Processing of Small Targets*. San Diego (CA, USA), SPIE, Aug 2005, p. 230–241. DOI: 10.1117/12.618730

[17] LI, P. Q., DENG, X. L., ZHANG, L. Y., et al. Sparse learning based on clustering by fast search and find of density peaks. *Multimedia Tools and Applications*, 2019, vol. 78, no. 23, p. 33261–33277. DOI: 10.1007/s11042-019-07885-7

[18] WANG, S. L., GAN, W. Y., LI, D. Y., et al. Data field for hierarchical clustering. *International Journal of Data Warehousing and Mining*, 2011, vol. 7, no. 4, p. 43–63. DOI: 10.4018/jdw.2011100103

- [19] WANG, S. L., WANG, D. K., LI, C. Y., et al. Clustering by fast search and find of density peaks with data field. *Chinese Journal of Electronics*, 2016, vol. 25, no. 3, p. 397–402. DOI: 10.1049/cje.2016.05.001
- [20] BARANY, I., VU, V. Central limit theorems for Gaussian polytopes. *Annals of Probability*, 2007, vol. 35, no. 4, p. 1593 to 1621. DOI: 10.1214/009117906000000791
- [21] GRANSTROM, K., ORGUNER, U. *Implementation of the GIW-PHD Filter*. Technical Report from the Automatic Control at Linköping Universitet, 2012, p. 1–9.
- [22] SCHUHMACHER, D., VO, B. T., VO, B. N. A consistent metric for performance evaluation of multi-object filters. *IEEE Transactions on Signal Processing*, 2008, vol. 56, no. 8, p. 3447 to 3457. DOI: 10.1109/TSP.2008.920469
- [23] ZHU, Y. Q., ZHOU, S. L., GAO, G., et al. Extended emitter target tracking using GM-PHD filter. *PLOS ONE*, 2014, vol. 9, no. 12, p. 1–18. DOI: 10.1371/journal.pone.0114317
- [24] GRANSTROM, K., ORGUNER, U. A PHD filter for tracking multiple extended targets using random matrices. *IEEE Transactions on Signal Processing*, 2012, vol. 60, no. 11, p. 5657–5671. DOI: 10.1109/TSP.2012.2212888

About the Authors ...

Yang GONG (corresponding author) was born in Suizhou, Hubei, China, in 1992. He received the B.S. and M.S. degrees from the Institute of Electronic Engineering, Hefei, China, in 2014 and 2016, respectively. He is currently pursuing the Ph.D. degree with the College of Electronic Engineering, National University of Defense Technology. His research interests include target tracking and adaptive signal processing.

Chen CUI was born in Yixian, Hebei, China, in 1962. He received the B.S. degree from the Institute of Electronic Engineering, Hefei, China, in 1984, and the M.S. degree from the University of Science and Technology of China, in 1991. He is currently a Professor with the College of Electronic Engineering, National University of Defense Technology. His research interests include adaptive signal processing, radar waveform design, and the signal processing in electronic countermeasures.